Aaltio, I.; Ge, Yanling; Pulkkinen, H.; Sjöberg, A.; Söderberg, O.; Liu, X.W.; Hannula, S.-P.

Crack growth of 10M Ni-Mn-Ga material in cyclic mechanical loading

Published in:
Physics Procedia

DOI:
10.1016/j.phpro.2010.11.080

Published: 01/01/2010

Document Version
Publisher's PDF, also known as Version of record

Available online at www.sciencedirect.com
ScienceDirect
Physics Procedia 10 (2010) 87–93
Physics Procedia
www.elsevier.com/locate/procedia

3rd International Symposium on Shape Memory Materials for Smart Systems

Crack growth of 10M Ni-Mn-Ga material in cyclic mechanical loading

I. Aaltio*, Y. Ge, H. Pulkkinen, A. Sjöberg, O. Söderberg, X.W. Liu, and S-P. Hannula

Aalto University, School of Science and Technology, Department of Materials Science and Engineering, P.O. Box 16200, FI-00076 Aalto, Finland

Abstract

The 10M martensitic Ni-Mn-Ga single crystal materials are usually applied in the magneto-mechanical actuators. Therefore, it is important to know the possible effect of the long-term cyclic shape changes on their structure and behavior. This can be evaluated with the mechanical fatigue testing. In the present study, the single crystal 10M Ni-Mn-Ga samples of different compositions were applied to strain-controlled uniaxial mechanical cycling in the multivariant state at ambient temperature. The experiments revealed distinctive changes of the twin variant structure, especially in the mobile twin area, density of twin boundaries, and in the tendency for fatigue crack growth. Characterization of the crack surface showed that the cracks in the microscale grow in a step-wise manner on specific crystallographic planes, i.e, twin boundary planes, but that the macroscopic crack does not occur only along crystallographic directions.

Keywords: magnetic shape memory; Ni-Mn-Ga; fatigue; cracking

1. Introduction

The five-layered modulated 10M martensitic Ni-Mn-Ga single crystals have attracted interest as magnetic shape memory (MSM) materials due to the high strains obtainable (6 %) [1]. Actuation results from the change of the magnetic-field-induced twin variant structure, in which the short axis (*c*) of the close-to-tetragonal martensite crystal lattice is aligned to the applied field direction, i.e. one twin variant changes or reorients to another [1-3]. This change is based on the high enough magnetic stress provided by large magnetic anisotropy of the material to move the twin boundaries in these alloys. They can be actuated at moderate applied magnetic field. This same shape change can be obtained also by external mechanical stress, when the low twinning stress needed to move the twin boundaries is exceeded. It is noteworthy that the twinning stress depends on the martensite variant structure in the

*Ilkka Aaltio, Tel.: +358 9 47022684
E-mail address: ilkka.aaltio@tkk.fi

1875-3892
doi:10.1016/j.phpro.2010.11.080

material; for example, in the single variant state more energy is needed to create the new secondary variant than in the multivariant state [4]. Therefore, the long-term actuation is not usually based on the maximum possible shape changes, but is restricted to the multivariant structure region. When these materials are used in dynamic actuation applications, their long term fatigue properties become increasingly important. Magneto-mechanical cycling of the seven-layered 14M materials is studied in [5,6], and some data exists also for the 10M materials [7-10]. These studies have shown that cycling generally decreases the obtainable magnetic-field-induced strain (MFIS) and promotes crack growth. In order to exclude the influence of the magnetic phenomena related to the actuator design on the long-term behavior, the present study is carried out on the 10M martensite using a purely mechanical, uniaxial tensile/compression loading as in [10].

In our previous work [10], fatigue properties of earlier batch than the present samples were studied. In [11], the manufacturer reported that the decreasing of impurities had resulted in a lowered twinning stress and increased instability of the twin structure. In this paper the fatigue performance of the low twinning stress 10M Ni-Mn-Ga samples is reported and compared with the performance of the earlier batch samples.

2. Experiments

The 10M samples (manufactured by Adaptamat Ltd., Finland) were applied to strain-controlled uniaxial mechanical cycling in the two variant state at ambient temperature. The rectangular samples had their edges along <100> directions. The chemical composition and static twinning stress were supplied by the manufacturer. The composition had been analysed by a specially calibrated x-ray fluorescence system (XRF) to ±0.1 wt-% and then converted to at-%.

The mechanical cycling test apparatus is described in [10]. It records the strain as peak-to-peak (%), twinning stress (MPa), and temperature (^{o}C) based on one hundred preceding loops, when the sampling frequency is 50 kHz. The tests in the present work were conducted under strain amplitude control or stress control (feedback) producing tension and compression in a sinusoidal waveform. More details of the samples and their testing are given in Table1.

Table 1. Tests samples and the details of the long-term fatigue test with the corresponding information from our previous work [ref. 10]. Samples with the same b-number are from the same fabrication batch. (*=dynamic value).

Sample	Ni (at%)	Mn (at%)	Ga (at%)	Control parameter	MFIS max. (static) (%)	Twin. stress (static) (MPa)	Strain (%, p-p)	Cycling frequency (Hz),	Max. nr of cycles	Working length (mm)	Sample dimensions (mm^3)
S1b1	50.0	28.3	21.7	Strain	6.0	0.2	0.5 - 2	300	n.a.	13.7	21.4x2.64x0.93
S2b2	50.4	28.0	21.6	Strain	6.4	0.11	1	300	$10.0x10^6$	5.0	11.7x2.29x0.96
S3b2				Load (1 MPa)	6.5		2.2-3.8	350	$3.7x10^6$	5.5	11.72x2.31x0.94
Ref. [10]	50.0	28.3	21.7	Load / strain	6.0	0.6 (*)	2	75-350	$>2x10^9$	11	20.1x2.5x1.0

At the beginning of the tests the twin variant structure of the samples was modified into fine state by bending, and then the samples were mechanically settled to a multivariant state (near to 50 % of [100] and [001] variant fractions). After setting the sample first to the fine-twin state by bending, and then to the two-variant state by a consequent compression, the variants in the center part of the sample had a tendency to coalesce into a coarse twin structure. In addition, one triangular variant having boundaries at approx. 45° to sample axis appeared into the S3b2 sample. Such instable variants were later found to influence the fatigue behavior of the sample. In the actual cycling test, the system was limited (mechanically and by software) in such a way that it restricted the sample from deforming into a single variant state.

Microstructural characterization of the samples was carried out by optical microscopy (Leica DMRX) using polarized light, and by XRD measurements (Philips X'Pert MRD Pro) using $Co_{K\alpha}$ radiation. Tranformation temperatures and the Curie point of the materials were established by magnetic susceptibility method. Scanning electron microscope (SEM LEO 1450) was applied for the detailed study of the fatigue cracks and fracture sufrace. The impurity levels in the present samples were too low for being reliably detected by EDS, and they were not examined further. Maximum magnetic field induced strain (MFIS) was measured as described in [10].

3. Behavior of the material in cycling

In the dynamic straining allowed by the twin boundary motion at martensite state, the hysteresis is basically due to the energy dissipation by internal friction [12,13]. The dissipated energy in the material is converted to heat, which is then conducted to the surrounding environment. Since a relatively high cycling frequency was used in the fatigue tests, heating of the sample in the (purely mechanical) fatigue test system as a function of strain amplitude was studied. Figure 1 shows the temperature of the sample S1b1 as a function of strain amplitude (%, p-p) at 300 Hz. The sample cooling was carried out as in the actual fatigue tests, but now temperature of the sample surface was measured with a thermocouple. The temperature increase of the sample during the cycling test is less than 2 K (Figure 1). Thus, the sample remains martensitic during the test, as its transformation temperatures (M_s = 315 K, M_f = 313 K, A_s = 318 K, A_f = 320 K) are clearly higher than the temperature at which the tests were carried out (296 K). Therefore, phase transformation is excluded from contributing to the observed structural changes or crack growth of the studied material.

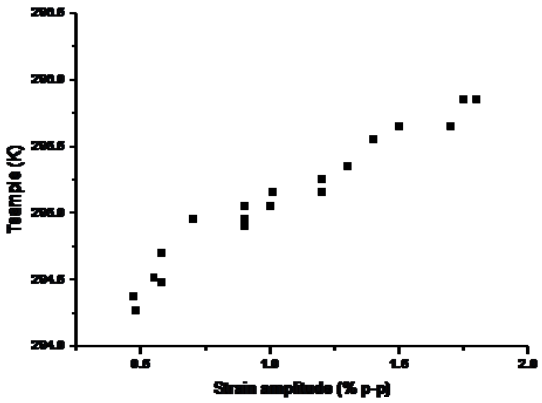

Figure 1. Temperature change of the sample S1b1 with increasing strain amplitude with cycling frequency of 300 Hz.

The evolution of the strain, stress and calculated twinning stress of the sample S2b2, together with the change of temperature of the specimen holder is shown in Figure 2. The applied sinusoidal load amplitude was in the beginning of the test slowly increased by the operator, and when the desired strain was obtained, it was set constant. The control system of the cycling apparatus then gradually increased the load amplitude from 1.7 to 2.2 MPa to attain the desired strain level. The gradual increase (change) of the twinning stress and applied stress amplitude correlates with the temperature decrease, since the twinning stress is temperature-dependent. The measured average twinning stress in the fatigue test was at a remarkably high level of 1.5 MPa and showed only slight increase during the cycling up to about 10.02 x 10^6 cycles, until the sample cracked. Before the fatigue test the twinning stress of the sample was statically measured to be 0.11 MPa, thus, the variation of the twinning stress is remarkable. Recent results [4] show that the twin structure of the sample may become interlocked in the single variant state. In [11] it was observed that the material prefers to adopt a single variant state. The interlocking was connected to the nucleation of a single twin boundary, and the twin structure could be released by magnetomechanical training. In

our experiments, the high initial level of the twinning stress suggests that the twin structure was interlocked even in the beginning of the cycling.

The front views of the S2b2 sample show a change in the twin variant structure of the sample (Figures 3a, 3c, and 3e). Comparison of the side views before cycling (Figure 3b), and after 10 x 10^6 cycles (Figure 3f) reveals that the twin boundaries have partly changed their orientation, and new inclined boundaries have appeared in the middle part of the stick at 90° angle towards the original boundaries. In this area, cracks have eventually appeared in cycling and at the same time there have appeared twin variant boundaries (Figure 3g).

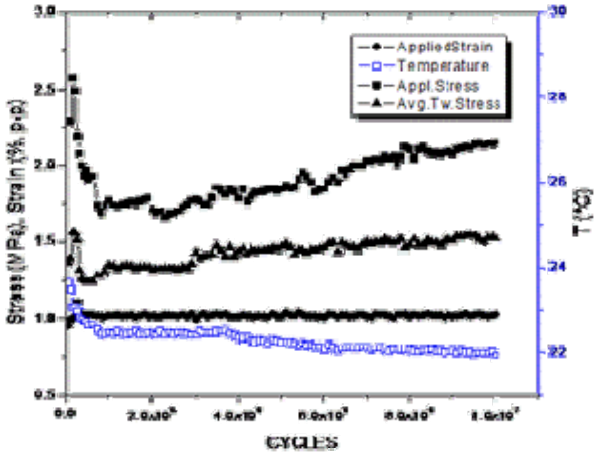

Figure 2. Strain (%, p-p), applied stress (MPa) and average estimated twinning stress (MPa) of the sample S2b2 during the cycling. Temperature is measured from the sample holder.

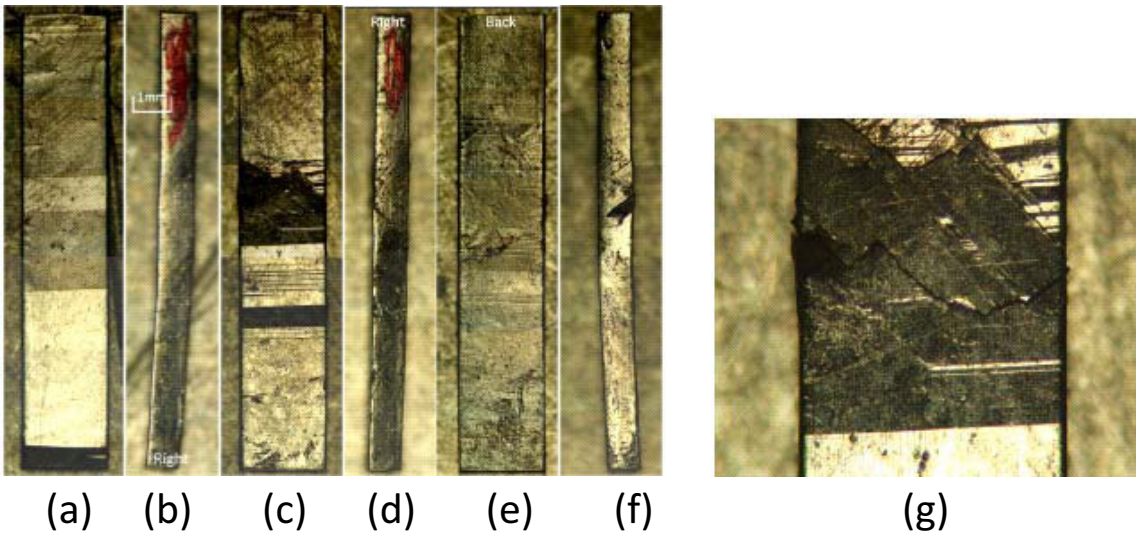

Figure 3. Twin structure of the sample S2b2 (a,b) before cycling, and (c-f) after 10.00 x10^6 cycles. Cycling axis is vertical in the figure. Sample width is 2.3 mm. (g) A detail of the cracked part of the sample after cycling.

The twin structure of sample S2b2 has been studied more in details by X-ray diffraction. The XRD line-scan was made with a beam size of 1x1 mm^2 along the centerline of the stick sample. This study showed that before the fatigue test the left side of the sample consists mainly coarse (100) twin variant, whereas at the right side of the sample has finer twin structure and more twin boundaries as both the (100) and (001) variants show higher intensity (Figure 4a). After the 10 x 10^6 cycles the corresponding XRD scan (Figure 4b) shows broader and more spread maxima-area for the (001) variant, while the strongest intensity for this variant is still in the same location as in the beginning. The spreading of the (004) peak is due to the refinement (i.e, increase of twin boundary density) of the twin structure by the cycling. When comparing the not cycled sample (Figure 3a) and the cycled sample (Figure 3c), the refining of the twin structure is seen.

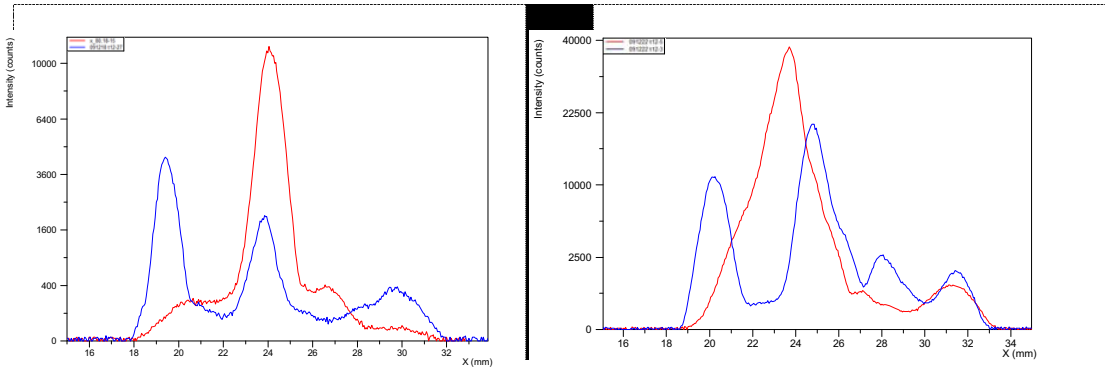

(a) (b)

Figure 4. The XRD line-scan along the sample length of the sample S2b2 (a) before cycling, and (b) after 10 x 10^6 cycles. In both cases, the (004) and (400) peak intensities are shown. The red pattern is connected to the (004), while the blue line shows the (400) peak intensity.

4. 4. Crack growth and fracture surface

The crack growth and surface cracking of the sample S2b2 was examined in details just before the final cracking of the sample, and then after the final fracture. Cracking occurred after 10.02 x 10^6 cycles in that part of the sample where the twin boundaries were mobile under external loading. Sample S3b2, which was cycled at load control, fracture by cracking in a similar way after 3.7 x 10^6 cycles. The crack growth observed on the surface of S2b2 after 10.00x10^6 cycles (Figure 4g), occurred macroscopically at 50 to 70° angle to the loading axis [001]. This differs from the orientation of the twin variants (89°) on the same surface, thus, the macroscopic crack was not growing along the moving twin boundaries.

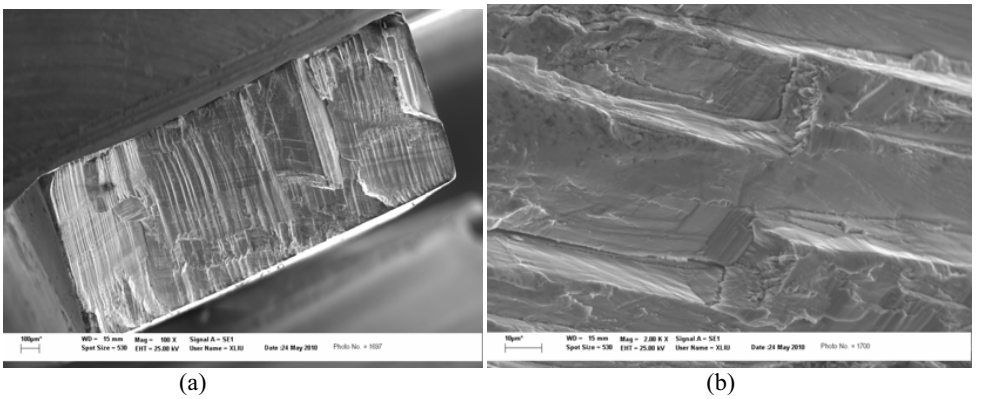

(a) (b)

Figure 5. The fracture surface overview of sample S2b2 (a) and a detail of the fracture surface (b), SEM SE images.

Near the stick edges, the cracks have propagated in more inclined direction relative to the loading axis than in the middle of the edges. It can also be noted that differently oriented twin variants have appeared at several locations beside the cracks. We suggest this to be a result of the change in the stress state of the sample due to the appeared crack, resulting in the accommodation of the twin structure. Figure 5a shows the final fracture surface of the sample. When observed at a larger magnification, it can be seen that the fracture has followed distinct planes i.e., twin boundary planes in a step-wise manner (Figure 5b) with variable step size. This is similar to the cracking reported in [10]. Facet like areas seen in Figure 5a, have obviously formed in a similar fashion. However, it seems that in those areas the crack has grown more continuously.

The narrow side surface of the sample S2b2 exhibits several cracks having the same direction (Figure 6a). On this side, the final fracture has the same orientation as the cracks beside it, and the macroscopic crack does not change its direction as it does on the wide face (Figure 4g).

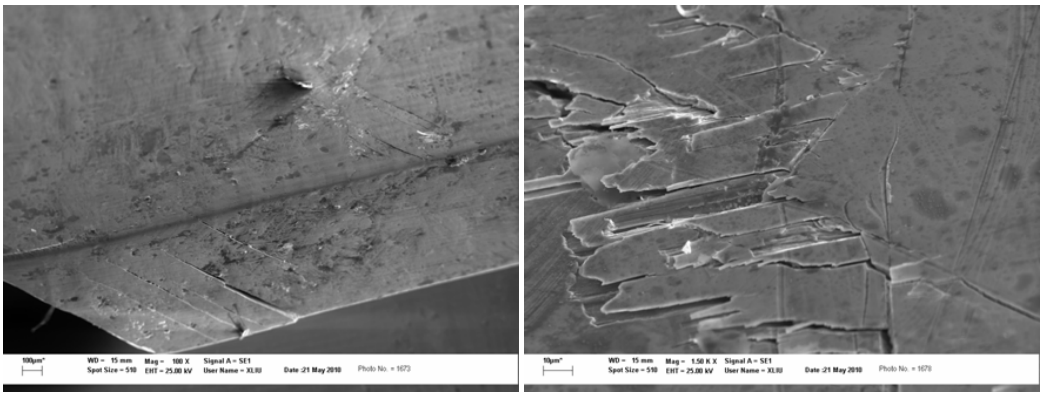

(a) (b)

Figure 6. (a) Side surfaces and cracks of the sample S2b2. The fracture surface is at left (dark). In (b) is a detail of the wedge-like cracking on the surface. SE.

The cycling had caused surface microcracking and chipping (Figure 6b). Similar features were found in the earlier cycled samples [10]. We propose this to be a result of the surface relief on the twin boundary, due to the shape change resulted by the different orientation ([100] and [001]) of the mainly tetragonal lattice. The shape change is expected to cause a sharp bend of the surface at the location of the twin boundary. When the twin boundary is driven back and forth, the bend will move with it. If the microstructure of the material contains parts which do not act in a similar way as the rest of the material (scratches with stress field, defects, e.g.), a stress concentration is expected to develop when the twin boundary passes through this area. A high enough stress can result in surface cracking at the respective area.

Fatigue life of the present samples was markedly lower (max. $10x10^6$ cycles) than that of the samples in the earlier production batch [10] (> $2x10^9$ cycles). The lower lifetime is expected taking into account the twin instability of the studied material with extremely low twinning stress. Similar twin instability of very low twinning stress material is reported in [11]. Since the studied material has a tendency to change from the fine-twin structure to a coarser one or the interlocking of the twin boundaries, stress transients or stress increase may appear in the fatigue sample, which can enhance the cracking. It is also probable that incompatible variants will form more often in this material than in the more steady and higher twinning stress Ni-Mn-Ga material, studied in [10].

5. 5. Conclusion

The results show that in mechanical high frequency cycling of 10M Ni-Mn-Ga MSM-material, fatigue crack nucleation and growth may take place in the material showing all the time only martensitic structure. The temperature of material may increase in mechanical cycling, but only couple of degrees, and thus, its influence on the fatigue behavior is minor. However, cycling changes strongly the twin structure resulting in increase of the

twinning stress. The fatigue life of the studied samples is clearly reduced when compared to less pure grade studied in [10]. This is proposed to be a result of the instability of the martensite twin structure which promotes cracking.

6. Acknowledgement

We wish to thank the Academy of Finland for supporting this research (FORMAFESMA project).

References

1. O. Söderberg, Y. Ge, A. Sozinov, S-P. Hannula, and V.K. Lindroos, in *Handbook of Magnetic Materials*, Amsterdam: Elsevier Vol. 16, pp.1-39, 2006.
2. R.C. O'Handley, and S.M. Allen, in *Encycl. of smart materials*, Schwartz, M (Ed.), Wiley, pp. 936-951, 2002.
3. I. Aaltio, O. Heczko, O. Söderberg, and S-P. Hannula, in *Smart Materials*, ed. M. Schwartz (Boca Raton: CRC Press Taylor & Francis) pp. 20-1…20-7, 2009.
4. I. Aaltio, O. Söderberg, Y. Ge, and S-P. Hannula, *Scripta Mat.* 62 (2010) 9.
5. P. Müllner, V.A. Chernenko, D. Mukherji, and G. Kostorz, *Mater. Res. Soc. Symp. Proc.* 785 (2004) 415.
6. M. Chmielius, V.A. Chernenko, W.B. Knowlton, G. Kostortz, and O. Müllner, *Eur. Phys. J Spec. Topics* 158 (2008) 79.
7. J. Tellinen, I. Suorsa A. Jääskeläinen, I. Aaltio and K. Ullakko *Proc. of ACTUATOR 2002*, pp.566-569, 2002.
8. O. Heczko, L. Straka, O. Söderberg, and S-P. Hannula, in *Proc. of SPIE* 5761 (2005) 513.
9. I. Aaltio, Y. Ge, X. Liu, O. Söderberg, J. Tellinen, A. Sozinov, and S-P. Hannula, in the International Conference on Martensitic Transformations, Santa Fe, New Mexico, USA, 29 June – 05 July 2008. *TMS special issue*, in press.
10. I. Aaltio, A. Soroka, Y. Ge, O. Söderberg, and S-P. Hannula, *Smart Materials and Structures* (2010), in press.
11. L. Straka, N. Lanska, K. Ullakko and A. Sozinov, *Appl. Phys. Lett.* 96 (2010) 131903.
12. V. G. Gavriljuk, O. Söderberg, V. V. Bliznuk, N. I. Glavatska and V. K. Lindroos, *Scripta Mat.* 49 (2003) 803.
13. J. Van Humbeeck, *J. Alloys Compounds* 355 (2003) 58.